Improvement of Inhibitors of the Macrophage Infectivity Potentiator Protein from *Trypanosoma cruzi*, *Burkholderia pseudomallei*, and *Legionella pneumophila* – a Comparison

Theresa Lohr[1], Carina Herbst[1], Nicole M. Bzdyl[2], Christopher Jenkins[3], Nicolas Julian Scheuplein[1], Wisely Oki Sugiarto[4], Jacob J. Whittaker[5*], Albert Guskov[5], Isobel Norville[3], Ute A. Hellmich[6, 7, 8], Felix Hausch[4,9], Mitali Sarkar-Tyson[2], Christoph Sotriffer[1], Ulrike Holzgrabe[1]

[1] Institute of Pharmacy and Food Chemistry, University of Würzburg, Am Hubland, 97074 Würzburg, Germany

[2] Marshall Centre for Infectious Diseases Research and Training, School of Biomedical Sciences, University of Western Australia, 35 Stirling Highway, 6009, Perth, Australia

[3] DSTL, Defence Science and Technology Laboratory, Porton Down, Salisbury, SP4 0JQ, United Kingdom

[4] Department of Chemistry and Biochemistry Clemens-Schöpf-Institute, Technical University Darmstadt, Alarich-Weiss Straße 4, 64287 Darmstadt, Germany

[5] Groningen Institute for Biomolecular Sciences and Biotechnology, University of Groningen, 9747AG Groningen, the Netherlands

[6] Institute of Organic Chemistry & Macromolecular Chemistry, Friedrich Schiller University Jena, Humboldtstraße 10, 07743 Jena, Germany

[7] Center for Biomolecular Magnetic Resonance, Goethe-University, Frankfurt/Main, Germany

[8] Cluster of Excellence "Balance of the Microverse", Friedrich Schiller University Jena, Jena, Germany

[9] Centre for Synthetic Biology, Technical University Darmstadt, 64287 Darmstadt, Germany

Corresponding Author: Prof. Dr. Ulrike Holzgrabe

ulrike.holzgrabe@uni-wuerzburg.de

Phone: 0049-931-3185461

*Current address: Department of Molecular Sciences, Swedish University of Agricultural Sciences, 75651, Uppsala, Sweden

Abstract

The treatment of Chagas disease and infections with Gram-negative bacteria is limited to a low number of antibiotics. Due to the development of resistance and partially severe side effects, there is an urgent need for new treatment strategies and virulence factors such as the macrophage infectivity potentiator (MIP) protein have emerged as a promising new therapeutic target. Inhibition of microbial MIP proteins leads to reduced viability and proliferation in pathogens such as *Legionella pneumophila* and *Burkholderia pseudomallei*. The parasitic pathogen of Chagas disease, *Trypanosoma cruzi*, also expresses a MIP protein, presumably involved in host cell invasion. Here, we took advantage of a compound library initially designed to inhibit MIPs of *Burkholderia* (*Bp*MIP) and *Legionella* (*Lp*MIP), to screen compounds against the *Trypanosoma*-MIP (*Tc*MIP). Using a fluorescence polarization assay (FPA), the first qualitative structure-activity relationships could be derived. Further compound development led to highly active inhibitors of all tested MIPs from pathogenic microorganisms. Docking studies, molecular dynamics simulations and quantum mechanical calculations suggest an extended σ-hole of the *meta*-halogenated phenyl sulfonamide to be responsible for the high affinity.

Keywords: Macrophage infectivity potentiator protein; *Burkholderia pseudomallei*, *Legionella pneumophila*, *Trypanosoma cruzi*; structure-activity relationship; quantum mechanical calculations

Introduction

The MIP proteins and the closely related MIP-like proteins are immunophilins, a widely distributed class of proteins. Within this group, the various MIP proteins from pathogenic microorganisms and the human FK506-binding proteins (hFKBPs) belong to the same superfamily of FK506-binding proteins (FKBPs), which are characterized by their peptidyl-prolyl *cis-trans* isomerase (PPIase) activity.[1] PPIases catalyze the rate-limiting reaction of protein-folding and are thus involved in numerous biological processes, such as signal transduction, gene regulation, protein secretion and tissue regeneration.[2, 3] Accordingly, MIPs from pathogens often contribute to virulence, classifying these proteins as virulence factors. MIPs have been functionally characterized for many Gram-negative bacteria, such as *Legionella pneumophila*[4, 5], *Burkholderia pseudomallei* [6, 7], *Neisseria* spp.[8], *Coxiella burnetii*[9], and *Klebsiella pneumoniae*[10]. In all these cases, the role of MIP in the penetration or survival of the pathogen in the host cell was demonstrated.[1] In addition to functional similarity, they also exhibit high sequence homology in their respective PPIase domains.[11] It is assumed that the inhibition of virulence factors, which are generally not essential for survival, suppresses the emergence of resistance, as is the case with antibiotics.[1] The bona fide inhibitor of FKBPs which gave this protein family its name, the macrolide lactone FK506, is used as an immunosuppressant, hence rendering it inappropriate for combating infectious diseases.[1, 3] Hence, non-immunosuppressive MIP inhibitors are of interest.

*Tc*MIP, the MIP protein of *Trypanosoma cruzi*, a kinetoplastid protozoan and the causative agent of Chagas disease, also called American trypanosomiasis, is one of the less well characterized MIP proteins. An estimated 8 million people are currently infected and approximately 20-30% develop a potentially life-threatening *T. cruzi* infection.[12] The only approved drugs for Chagas treatment are nifurtimox and benznidazole, which besides from having severe side effects, are rather limited to the administration in the acute phase of the disease.[13] New strategies to combat Chagas infections are therefore urgently needed. In the infective stage of the parasitic life cycle, trypomastigotes secrete the *Tc*MIP protein.[14] *Tc*MIP promotes the productive infection of epithelial cells with *T. cruzi* and pre-treatment of rhesus monkey kidney epithelial (LLC-MK_2) cells with *Tc*MIP leads to a four-fold increase in the number of internalized parasites.[11] Encouragingly, the invasive effect can be reversed either by antibodies against *Tc*MIP or a low dosage of FK506,[14] establishing *Tc*MIP as a promising drug target to combat Chagas disease.

Due to the broad spectrum of MIP activity, there are numerous efforts to develop small molecule inhibitors for these targets.[3] The approaches are derived from the natural products rapamycin and FK506. As the corresponding small-molecule inhibitors lack the so-called effector domain that induces immunosuppression in humans, they are appropriate for anti-infective therapy.[15] For example, Pomplun et al. developed structurally related compounds, with an (*S*)-C^5-substituted [4.3.1]-aza-amide bicycle, which showed inhibitory activity in vitro against MIPs of the pathogens *Plasmodium falciparum* and *Chlamydia trachomatis*.[16] Wiedemann et al. could establish the structural basis of [[4.3.1]-aza-bicyclic

sulfonamide binding to *Lp*MIP and *Tc*MIP.[17] Scheuplein et al.[18] and Seufert et al.[19] designed a compound library of *B. pseudomallei* and *L. pneumophila* MIP inhibitors which are derived from the pipecolic moiety of the FK506 (see **Fig 1**. Entry 1). These pipecolic-acid derived inhibitors are effective in the nanomolar range with enhanced drug-likeness and do not show immunosuppressive properties.[15, 18] Moreover, the introduction of a side chain, in the linker between the two carbonyl moieties (see **Fig. 1**, Entry 2 and 3), significantly improves inhibitory activity towards MIPs of *B. pseudomallei* and *Neisseria spp*.[18] The affinity of the compounds towards *Bp*MIP was determined by means of a fluorescence polarization assay (FPA) reported before (see **Fig. 1**).[18, 20] Additionally, the inhibition of the prolyl-peptidyl-*cis, trans*-isomerase (PPIase) activity, the relevant enzymatic property of MIPs, was evaluated.[18, 20] In both assays, the compounds characterized by an *S,S*-configuration performed best. Studying the broad spectrum of activity of pipecolic acid-derived MIP inhibitors, Debowski et al. could show that these compounds effectively extend the survival of *Galleria mellonella* infected with *C. burnetti*, a Gram-negative bacterial pathogen, indicating *in vivo* activity of MIP inhibitors.[9]

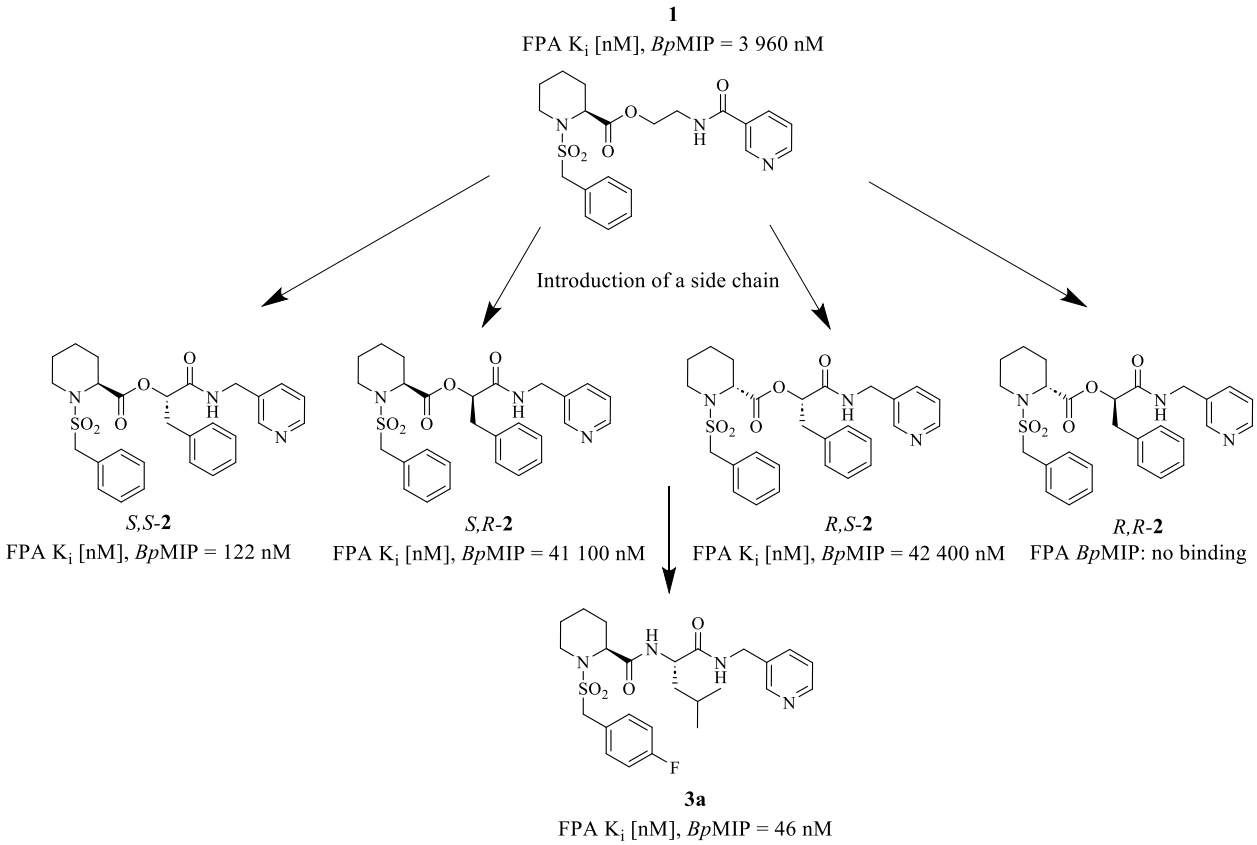

Figure 1: Previously described MIP inhibitors, derived from **1**, and K_i values determined by the fluorescence polarization assay (FPA) using *Bp*MIP. The inhibitors *S,S*-**2**, *S,R*-**2**, *R,R*-**2** and *R,S*-**2** differ only in their configuration with *S,S*-**2** being the preferred isomer, as all the others show low or no binding (n.b.) in the FPA screening. **3a** is a hit compound for *B. pseudomallei* MIP first described by Scheuplein et al.[18]

In this study, based on their prior performance against *Burkholderia*-MIP, we chose hit compounds **1**, i.e. the isomers of **2**, and **3a** (**Fig. 1**) as the starting point for extension of the activity profile to *T. cruzi* and the development of new pan-MIP inhibitors for *Tc*MIP, *Lp*MIP and *Bp*MIP. A newly synthesized compound library was tested with FPA against purified *Trypanosoma*- and *Legionella*-MIP. the respective structure-activity relationships (SARs) were determined using *Bp*-, *Lp*-, and *Tc*MIP binding and PPIase activity inhibition assays. In addition, the *in vivo* activity of one representative compound was assessed in a *Galleria mellonella* infection model. Importantly, we obtained inhibitors with increased affinity for *Tc*MIP, which was further substantiated by docking studies, molecular dynamics (MD) simulations and quantum mechanical calculations.

Results and Discussion

Expansion of the Previously Described Compound Library

The binding affinities to MIP proteins were determined by means of the previously developed FPA according to Scheuplein, Lohr et al.[20] This assay represents a rapid and robust screening method for MIP inhibitors with high consistency of results with the conventionally used PPIase assay.[20] In the FPA, the dissociation constant (K_D) value of a fluorescent probe (here: probe **A** or probe **B**, see SI) can be determined directly. In contrast, the compound screening is based on competition of the respective inhibitor with this probe. The inhibitor is added to a defined concentration of protein preincubated with the probe. The inhibitor affinity is eventually determined by replacement of the probe indicated by the decrease in fluorescence polarization value. Based on this, the K_i value can be calculated according to Wang et al.[21]

The pipecolic acid inhibitors **1** – **2**, whose affinity for *Bp*MIP was demonstrated by Scheuplein et al.[18] (**Fig. 1**) were tested against *Bp*MIP, *Lp*MIP and *Tc*MIP to identify a starting point for the development of new and more effective MIP inhibitors. Of note, only the PPIase domain of *Lp*MIP was used here, i.e. residues 77-213. Examination of the binding behaviour of the previously described compounds **1** – **2** reveals that the affinity to the *Bp*MIP protein is generally highest compared to *Tc*MIP and *Lp*MIP (**Table 1**), with K_i value of the former lead compound **1** in the micromolar range. Upon introduction of a benzyl side chain,[18] only the inhibitor with an *S,S*-configuration shows a considerable increase in binding affinity, whereas the other isomers were far less affine or showed no binding to the MIP proteins. The results of the FPA were comparable for all three MIPs, although higher affinities of the *S,S*-enantiomer to *Bp*MIP and *Tc*MIP compared to *Lp*MIP were observed.

Table 1: Compounds previously shown to be effective against *Bp*MIP[18] were tested against *Tc*MIP and *Lp*MIP-PPIase domain (residues 77-213). K_i values were determined by the fluorescence polarization assay and are given as the mean of at least three independent measurements. Raw data and standard deviation are given in the supporting information (SI).

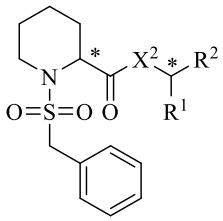

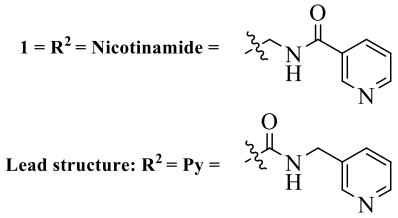

Inhibitor	*Config. at Pipecolic acid* *	Side chain	*Config Side chain* *	X²	R²	FPA K_i [nM], *Bp*MIP[18]	FPA K_i [nM], *Tc*MIP	FPA K_i [nM], *Lp*MIP-PPIase
1	*S*	-	-	O	**Nicotinamide**	**3 960**	**91 300**	**97 000**
S,R-**2**	*S*	*Bn*	*R*	O	**Py**	**41 100**	**n.b.***	**n.b.***
S,S-**2**	*S*	*Bn*	*S*	O	**Py**	**122**	**209**	**1710**
R,R-**2**	*R*	*Bn*	*R*	O	**Py**	**n.b.***	**n.b.***	**n.b.***
R,S-**2**	*R*	*Bn*	*S*	O	**Py**	**42 400**	**n.b.***	**n.b.***

* n.b. (no binding)

Based on compounds **1 - 2**, an expansion of the compound library was created, which contains two variations of a side chain that can be synthetically traced to the amino acids *L*-leucine (*Leu,* **3a**) and *L*-methionine (*Met,* **3b**). Additionally, the benzyl substituent of the sulfonamide was replaced with a phenyl ring. Since in previous studies a substitution with an amino- or nitro- group was found to reduce the affinity,[22] *p*-F, *m,p*-Cl,Cl, *m*-Br and *m,m*-Cl,Cl, were introduced here. Additionally, a *m,p*-Cl,Cl (**4a**) substitution pattern of a benzyl moiety was considered. The compounds are shown in **Figure 2**.

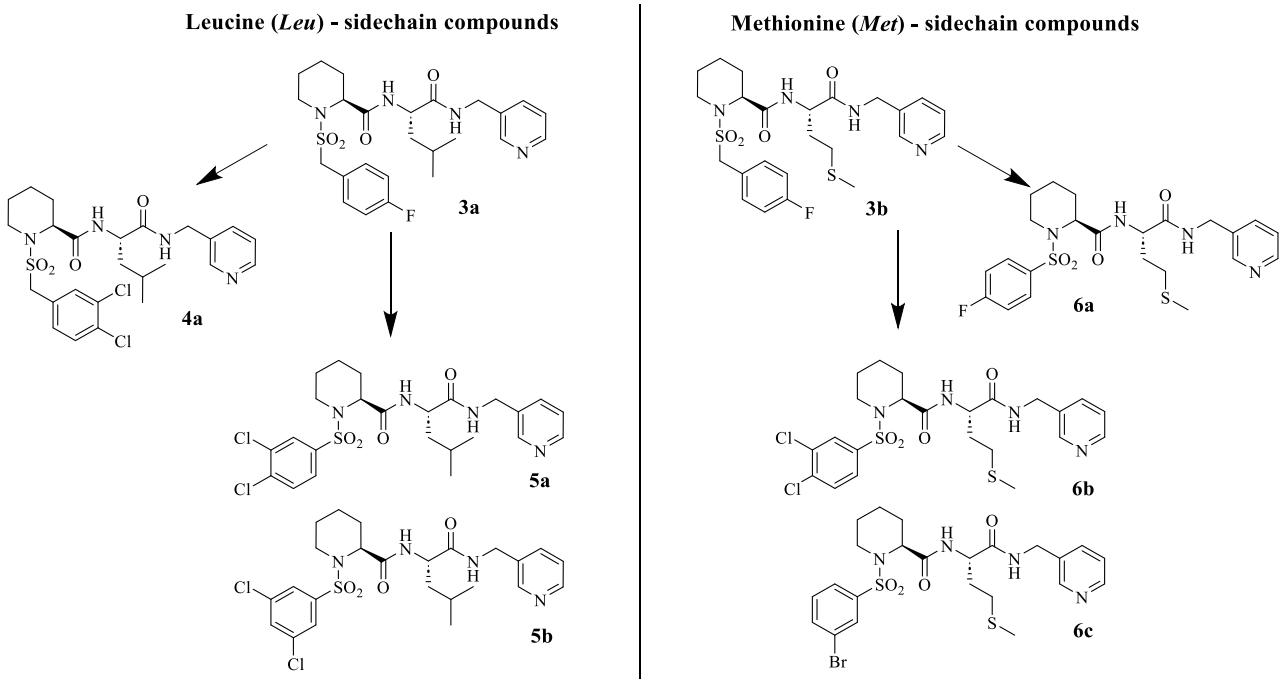

Figure 2: The compound library based on *Leu*- or *Met* expansions of the lead molecule **1**. Omission the methylene group of the sulfonamide residue result in **6a** and different halogen substitution in **4a** follow. **6b**, **6c**, **5a**, and **5b** represent combinations of these modifications.

Following the protocol established by Scheuplein et al.[18], a synthetic route was chosen that allowed the late variation of the sulfonamide residue and the formation of stereochemically pure pipecolic acid amide derivatives. Starting from the commercially available Boc-protected amino acids *L*-leucine or *L*-methionine, a coupling reaction was carried out with 3-picolylamine using *O*-(benzotriazol-1-yl)-*N*,*N*,*N*′,*N*′-tetramethyluronium-hexafluorophosphat (HBTU) and *N*,*N*-diisopropylethylamin (DIPEA). Subsequently, the *tert*-butyloxycarbonyl (Boc)-protection group was removed with an excess of trifluoroacetic acid (TFA), resulting in the amides **7a** and **7b**. Further coupling with Boc-*S*-pipecolic acid and deprotection under the same conditions gave the intermediates **8a** and **8b**. The sulfonamides (**3b**,**4a**, **5a**, **5b**, **6a**, **6b**, **6c**) were formed using the respective sulfonyl chloride derivative.

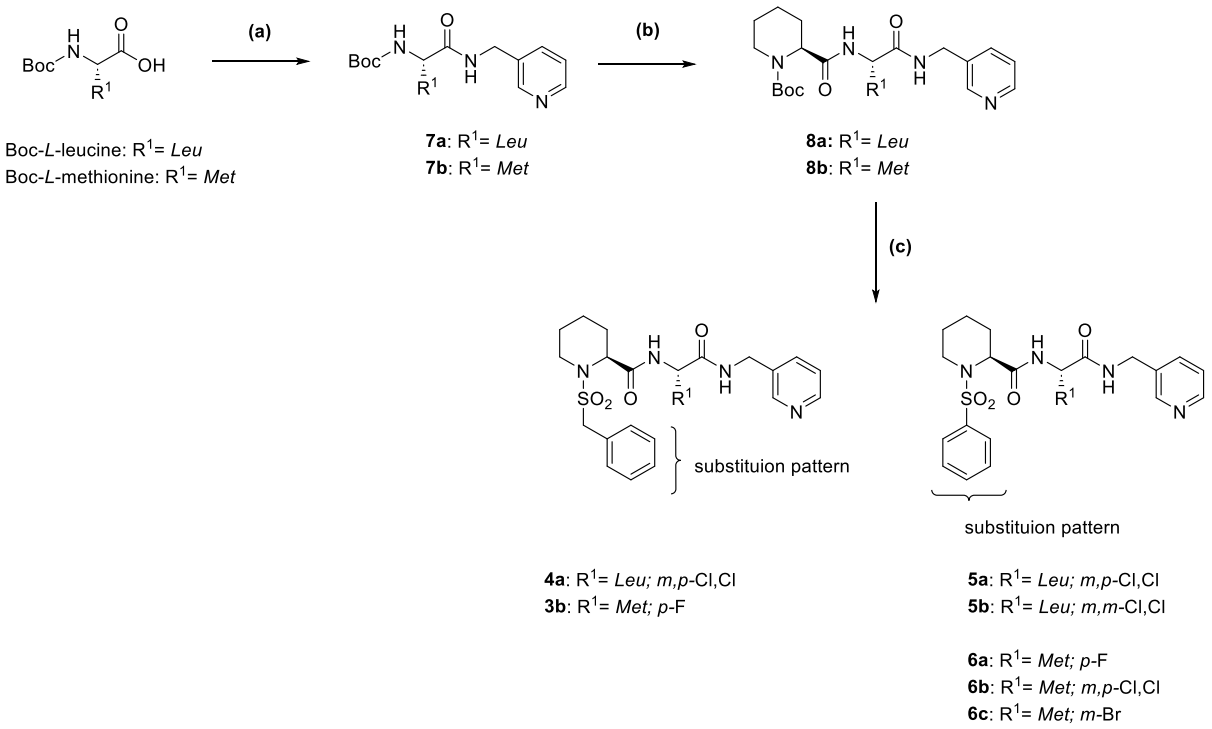

Scheme 1: Synthesis scheme of stereochemically pure compounds.
Reagents and conditions: (**a**) 3-picolylamine, HBTU, DIPEA, dichloromethane (DCM)/*N*,*N*-dimethylformamide (DMF), 0°C → rt; (**b**) i) TFA, 0°C → rt; ii) *N*-Boc-(*S*)-pipecolic acid, HBTU, DIPEA, DCM/DMF, 0°C → rt; (**c**) i) TFA, 0°C → rt; ii) correspondingly substituted phenylmethanesulfonyl chlorides or substituted benzenesulfonyl chlorides, triethylamine (TEA), DCM, 0°C → rt.

Furthermore, **10**, the *N*-Oxide of **5b**, being the metabolite,[23] as well as the mono-ester compound **11** with 3,5-dichlorobenzyl residue, but without a side chain, were synthesized (**Scheme 2**). To form the pyridine-*N*-Oxide (**10**), **5b** was treated with *meta*-chloroperoxybenzoic acid (*m*-CPBA). **11** was synthesized starting from the amine **12**, using 3,5-dichlorobenzenesulfonyl chlorides and TEA.

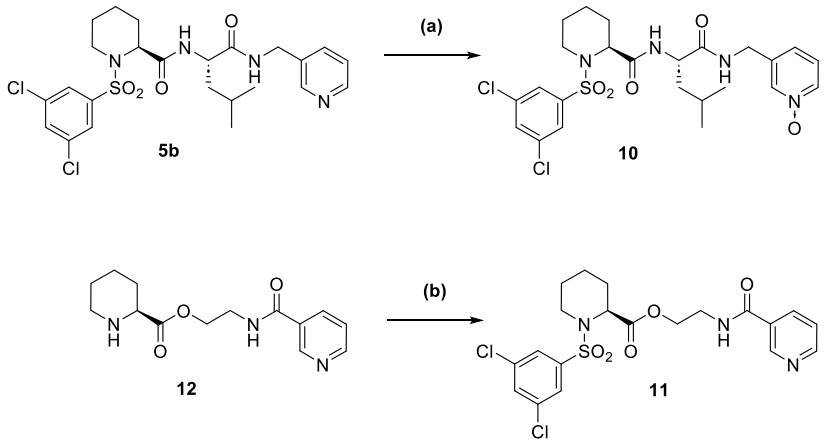

Scheme 2: Compound **10** is the *N*-Oxide and thus the main metabolite of **5b**.[23] To further estimate the influence of the 3,5-dichlorobenzyl residue, an inhibitor (**11**), similar to **1**, without a side chain, carrying this residue was investigated.

Reagents and conditions: (a) *m*-CPBA, EA, 0°C; (b) 3,5-Dichlorobenzenesulfonyl chlorides, TEA, DCM, 0°C → rt.

Structure-Activity Relationships by FPA Screening

The FPA results obtained for *Tc*MIP, *Bp*MIP and *Lp*MIP are displayed in **Table 2**. Almost all compounds were found to show affinity to the MIP protein. In general, the affinity of all compounds is about ten-times higher for *Bp*MIP than for *Tc*MIP and about a hundred-times higher than for *Lp*MIP. For the most potent compounds, the inhibition of the Bp-PPIase activity was additionally measured at 400 nM of inhibitor using the protease-coupled PPIase assay.[20] Common to all MIPs was the observation that compounds with a leucine-derived side chain exhibited a higher affinity than the methionine-derived ones. Furthermore, the ester compound **11** without side chain shows almost no affinity to the MIPs. Previous findings indicated the superiority of the bisamide linked compounds, not only with regard to affinity, but also in terms of chemical stability.[18]

Furthermore, the compounds characterized by phenyl substitution at the sulfonamide group generally showed higher affinity to the MIPs than the benzyl substituted ones, which have been reported by Scheuplein et al.[18] Since the only exception is the *p*-F-benzyl compound **3b**, which shows an affinity similar to the *p*-F-phenyl substituted substance **6a**, it stands to reason that the substitution at this residue has a major influence on the binding affinity. In contrast to amino- and nitro-phenyl substituted compounds, reported in previous studies[22] as poor inhibitors of the PPIase activity of *Lp*MIP, the halogen substituted compounds led to a one/two-digit nanomolar affinity, especially for the interaction with *Bp*MIP. These results are highly consistent with the results of the PPIase assay for *Bp*MIP (see **Table 2**). A comparison of the benzyl-substituted inhibitors **3a** and **4a** revealed that the deletion of the methylene group between the pipecolic acid nitrogen and the sulfonamide moiety is key for binding to *Tc*MIP and *Lp*MIP, whereas *Bp*MIP has a greater tolerance towards the methylene group.

Table 2: Screening of compounds with modifications of the side chain (code: *Met* or *Leu*) and of the sulfonamide residue (X^1), with or without methylene group and different halogen substitution. The K_i values were determined using FPA and represent a series of at least three independent measurements. For *Bp*MIP, the percentage of remaining activity relative to the dimethyl sulfoxide (DMSO)-treated recombinant protein was calculated. Raw data are given in the SI.

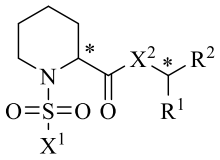

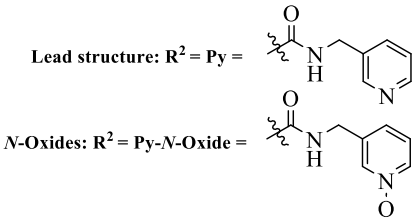

Inhibitor	*Subst. at X¹*	*Methylene at X¹*	X^1	X^2	Side chain Code	R^2	FPA K_i [nM], *Bp*MIP	*Bp*MIP % K_{obs} remaining at 400 nM inh.,	FPA K_i [nM], *Tc*MIP	FPA K_i [nM], *Lp*MIP-PPIase
3b	*p*	✓		NH	*Met*	**Py**	**98**	**n.d.**	**1 330**	**6 980**
6a	*p*	*X*		NH	*Met*	**Py**	**40**	**n.d.**	**1 960**	**6 120**
6b	*m, p*	*X*		NH	*Met*	**Py**	**2**	**1.2**	**40**	**430**
6c	*m*	*X*		NH	*Met*	**Py**	**4**	**2.7**	**105**	**448**
3a	*p*	✓		NH	*Leu*	**Py**	**46**[18]	**5.4**	**389**	**3 250**
4a	*m, p*	✓		NH	*Leu*	**Py**	**9**	**3.0**	**350**	**3 250**
5a	*m, p*	*X*		NH	*Leu*	**Py**	**3**	**1.6**	**5**	**293**
5b	*m, m*	*X*		NH	*Leu*	**Py**	**1**	**1.1**	**6**	**82**
10	*m, m*	*X*		NH	*Leu*	**Py-*N*-Oxide**	**19**	**3.1**	**264**	**1 020**
11	*m, m*	*X*		O	---	**Py**	**467**	**n.d.**	**7 630**	**43 100**

Whereas most compounds of our library (cf. **Table 1** and **2**, and other compounds not shown here) did not show any or only very low affinity to *Tc*MIP and *Lp*MIP, compound **5b** is the first inhibitor with an excellent affinity to all MIPs.

To explore the toxicity of this molecule *in vivo*, **5b** and its main metabolite[23] **10** were injected into five *Galleria mellonella* larvae at a concentration of 100 µM or 500 µM. Of note, due to solubility issues, compound **10** rather than the most effective in vitro MIP inhibitor was chosen. All larvae survived for 5 days, so that the compounds can be considered non-cytotoxic, which is consistent with previously published data for the lead compounds **1**, **2** and **3a** on NIH3T3- and HEK293T-cell lines.[18]

To investigate a possible *in vivo* activity, the *N*-Oxide **10** of hit compound **5b** was screened in a *Galleria mellonella* infection model with *B. thailandensis,* as a model pathogen for *B. pseudomallei.* In a previous

experiment, it was shown to behave similarly to *B. pseudomallei*.[24, 25] Nonetheless, it needs to be noted that in general *Galleria* are rather sensitive to *Burkholderia* infections, which may influences the significance of the study. Groups of 10 larvae were infected with *B. thailandensis.* After 2 hours, 10 µl of a combination of cotrimoxazole (10 mg/kg) and MIP inhibitor (250 µM) was applied. The addition of an antibiotic is required because MIP inhibition is not expected to eradicate the pathogens due to MIPs' non-essential nature.[1] Uninfected larvae (treated with phosphate-buffered saline, i.e. the 'PBS group') and those that had only received cotrimoxazole or diluent were used as controls. As seen in **Fig.3**, uninfected *Galleria* showed a survival percentage of 100 percent, whereas infected *Galleria* treated with only the diluent died quickly. Interestingly, the infected *Galleria* treated with the combination of cotrimoxazole and the *N*-Oxide **10** showed a slightly better survival rate than the *Galleria* treated with only the antibiotic. This suggests that inhibition of MIP can be beneficial for the infected host.

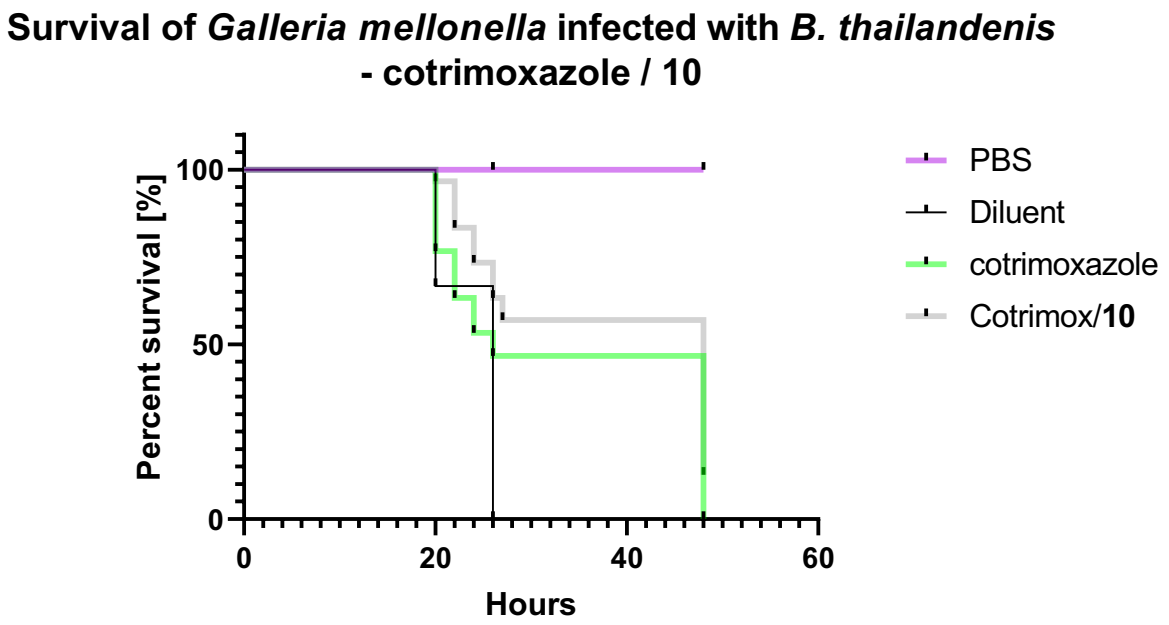

Figure 3*:* Survival of *G. mellonella* infected with *B.thailandensis* after treatment with a combination of cotrimoxazole (10 mg/kg) and MIP inhibitor **10** (250 µM) or cotrimoxazole alone. Uninfected *Galleria* (PBS) and untreated *Galleria* (diluent) serve as reference groups.

Computer-Assisted Analysis of Structure-Activity Relationships

To elucidate the reason of the enhanced binding affinity observed for compounds with a truncated and *meta*-halogenated sulfonamide residue in conjunction with a side chain group, molecular docking analyses with *Tc*MIP were conducted for all compounds shown in **Figure 2**. The docking protocol was adapted from Seufert et al.[19] and allowed the reproduction of the conserved structural moieties compared to the crystallographically observed binding mode as shown in **Figure 4a** and **Figure S1**. The

positioning of the halogenated phenyl group near the flexible loop suggested that a halogen bond may be formed upon ligand binding. Focusing on the example of compound **5b** and *Tc*MIP, the carbonyl oxygen of Gly122 could be a potential interaction partner. However, a hypothetical halogen bond would need to compete with the intramolecular hydrogen bond present in the flexible loop of the *Tc*MIP crystal structure in complex with **3a** (PDB: 8P42) between Gly122 and Ile126.[26]

Following up on this hypothesis, molecular dynamics simulations were employed with Schrödinger's Desmond[27, 28] and the OPLS4 force field[29], which applies off-centered point charges to represent σ-holes. Assessment of the obtained trajectories could indeed confirm the repeated occurrence of a σ-hole interaction as shown in **Figure 4b**. In the respective analyses, a halogen bond was considered to be present if, first, the X-O distance between halogen and carbonyl oxygen was within the range of 3.0 to 3.4 Å for chlorine, or 3.0 to 3.5 Å for bromine as proposed by Bissantz et al.;[30] and, second, the C-X-O angle exceeded 150°, indicating whether the oxygen atom is pointing in the direction of the σ-hole of the halogen atom.[31] In the three replicas of 100 ns MD runs with compound **5b** and *Tc*MIP, the occurrence of a halogen bond was observed in 19.4%, 14.7%, and 19.9% of the frames, respectively. Results of the MD runs with the other inhibitors are provided in **Table S4**. While the approximation of σ-holes through element-specific off-centered point charges is a well-established concept in molecular dynamics simulations[32], it is essential to note that this approach is only a very rough approximation of the actual electronic circumstances. Therefore, it does not allow any quantitative comparison of different ligands.

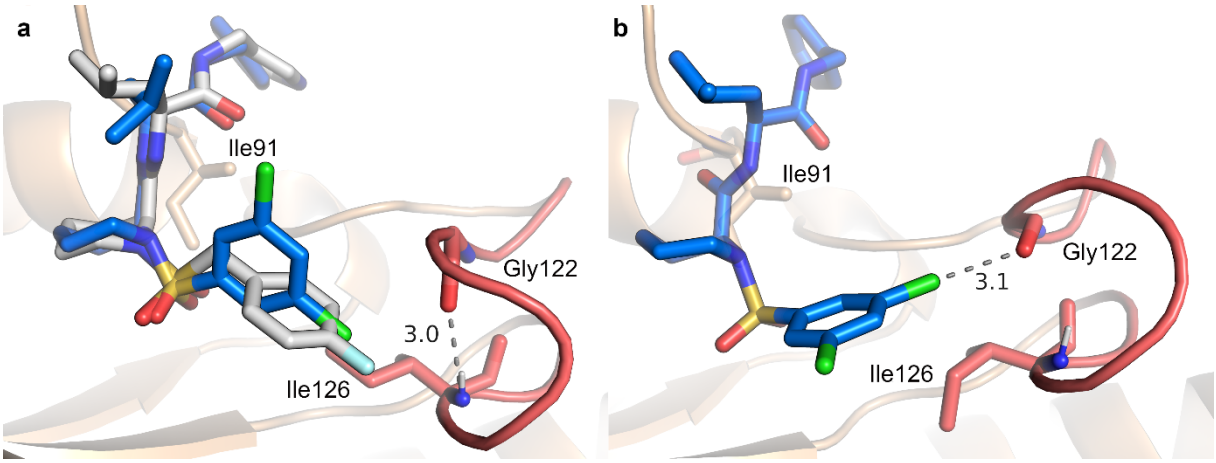

Figure 4: (a) The docking pose of compound **5b** (in blue) is in accordance with the binding position observed in the crystal structure of *Tc*MIP in complex with compound **3a** (PDB: 8P42)[26] *Tc*MIP in beige, ligand in grey). The flexible loop is highlighted in red. (b) Snapshot from the MD simulation of compound **5b** with *Tc*MIP at 31.76 ns. The formation of a halogen bond with carbonyl oxygen of Gly122 can be observed.

For a more detailed analysis of the electrostatic surface potential, quantum mechanical calculations (DFT, B3LYP/6-311+G**) on substructures of the inhibitors containing either chlorine or bromine were conducted. The results are illustrated in **Figure 5**. When the benzyl group is truncated to a phenyl

moiety, the extent of the corresponding σ-hole is amplified significantly due to the -M effect of the adjacent sulfonamide group. Since the extent of the σ-hole has a considerable impact on the potential energy gain from a halogen bond, it does not surprise that inhibitors with a shortened and meta-halogenated sulfonamide residue demonstrated improved binding affinity in this study.

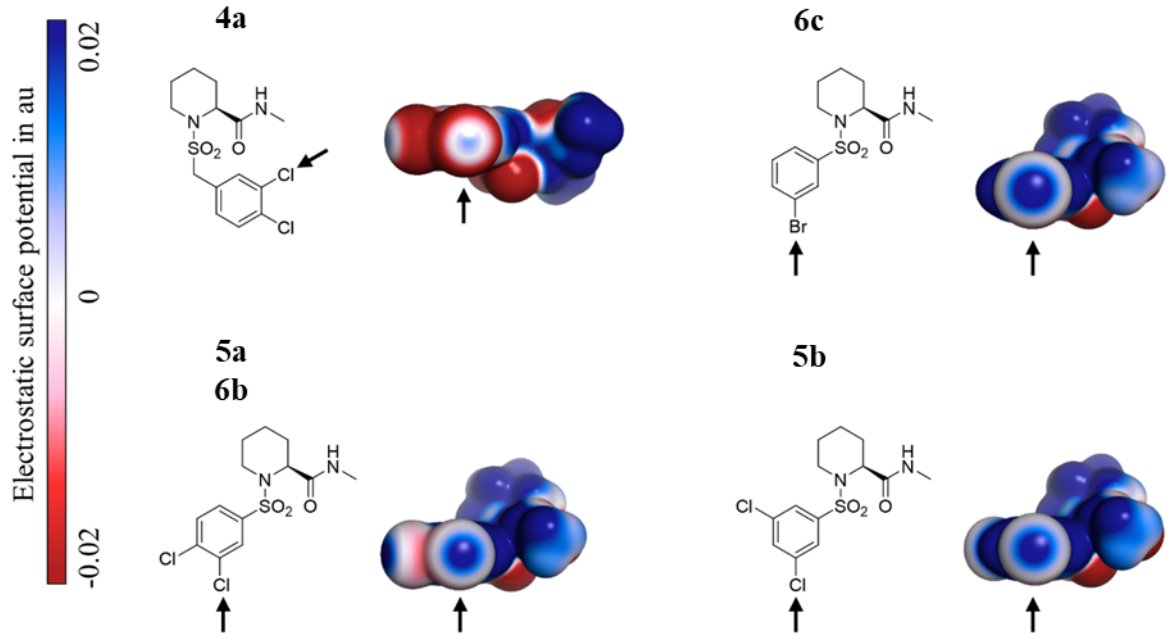

Figure 5: Calculation (B3LYP/6-311+G**) of the electrostatic surface potential with substructures of the inhibitors reveals major differences in the magnitude of the σ-holes. The arrows indicate the viewing angles.

Affinity of the MIP Inhibitors to hFKBPs

For the therapeutic use of MIP inhibitors, interaction with human FKBPs (hFKBPs) must be considered. Due to the high homology of the proteins in the active site, selectivity for one of the targets is extremely unlikely. Nevertheless, a preference for the desired target is recommended with regard to *in vivo* application. The human FKBPs (FKBP12, FKBP12.6, FKBP51 and FKBP52) differ in their size and function in the human organism and were examined in a FPA according to Bauder et al.[33] The lead compounds **3a** and **3b** show the following ranking in terms of their binding affinity: FKBP12 ≥ FKBP12.6 > FKBP51 > FKBP52. While no higher affinity to *Tc*MIP could be achieved for the first two lead compounds, *Bp*MIP shows a 2 to 3-fold superiority compared to the K_i-value of FKBP12. Even if there is no selectivity to the pathogenic MIP, the data can be used to make an assessment of the influence on human FKBPs.

Table 3: K_i-values of the initial lead compounds **3a** and **3b**, values are given as mean from two independent measurements using FPA.[33, 34]

hFKBP / Compound	FKBP51	FKPB52	FKBP12.6	FKBP12	For comparison: *Tc*MIP	For comparison: *Bp*MIP
3a	3130	1600	122	82	389	46
3b	15 740	2350	230	271	1 330	98

Conclusion

The compound screening revealed novel structure-activity relationships for all three pathogenic MIP proteins and further emphasizes the structural similarity of the MIP proteins, regardless of taxonomic origin. High-affinity inhibitors were identified for all target proteins, and although there is no selectivity to individual MIPs, key structural moieties for targeting the active site of MIPs have been revealed. Moreover, the extent of enhancement differs with the particular modification, providing new starting points for optimized inhibitors. Docking, MD simulations and quantum mechanical calculations offer a reasonable explanation for the improvement of binding affinity and help to understand the inhibitor-protein interactions. Accordingly, only the *meta*-halogen substitution in combination with a phenyl residue at the sulfonamide allows interaction with the flexible loop. An amino- or nitro-group does not provide the prerequisite for a σ-hole interaction, which furthermore explains the earlier results. In summary, the MIP inhibitors have been refined into highly potent, broad-spectrum and non-cytotoxic compounds ready for detailed *in vivo* testing.

Experimental Section

Organic Synthesis

General experimental procedures and equipment

The following general experimental procedures and equipment were according to Scheuplein et al.[18]

General. Common chemicals and reagents were purchased from *Alfa Aesar* (Ward Hill, USA), *Merck* (Darmstadt, Germany), *Avantor* (Darmstadt, Germany), *TCI Deutschland GmbH* (Eschborn, Germany), *Fisher Scientific* (Schwerte, Germany), and *ABCR* (Karlsruhe, Germany). They were used without further purification.

Gravity-driven column chromatography. Silica gel 60 (0.063-0.200 nm) from *Merck* (Darmstadt, Germany) was used for gravity column chromatography. Solvent composition is specified for each compound in the synthesis section.

TLC. Thin layer chromatography (TLC) was carried out on pre-coated silica gel glass plates SIL G-25 Spots were identified by irradiation and subsequent fluorescence quenching at 254 nm or excitation at 366 nm.

Mass spectrometry. Electrospray ionization (ESI) mass spectra were measured with a *Shimadzu LCMS-2020* (*Shimadzu Scientific instruments*, Kyoto, Japan). Data are reported as mass-to-charge ratio (m/z) of the respective positively charged molecular ions. Chromatographic method is given in SI.

High-Resolution Mass Spectrometry. High-resolution mass spectrometry (HRMS) was performed using an *Agilent* Infinity II LC-system (Waldbronn, Germany), equipped with a *Sciex* X500R QTOF mass spectrometer (Concord, Ontario, Canada) and a Turbo V^{TM} Ion Source (ESI). Chromatographic method is according to Scheuplein et al.[18]

Infrared Spectrometry (IR). IR spectra were recorded on a Jasco-FT-IR-6100 system (*Jasco Deutschland GmbH*, Groß-Umstadt, Germany) equipped with a diamond ATR accessory. The wave numbers of characteristic absorption bands are given in [cm^{-1}].

Nuclear Magnetic Resonance Spectroscopy. ^{1}H (400.132 MHz) and ^{13}C (100.613 MHz) NMR spectra were recorded on a Bruker AV 400 instrument (*Bruker Biospin*, Ettlingen, Germany). Topspin® (version 3.2-pl7) software (*Bruker Biospin*, Ettlingen, Germany) was applied for processing of NMR spectra.

Melting points. To determine melting points, an MP70 melting point system (*Mettler-Toledo GmbH*, Gießen, Germany) was used.

Purity. All purities of the compounds were verified by high-performance liquid chromatography (HPLC). All final compounds synthesized had purities above 95%. Purity data and HPLC methods are given in the SI.

Solubility. Thermodynamic solubility was determined for **5b** and **10** by using the continuous shake flask protocol of Hiltensperger et al.[35]

Substances known from literature. Synthesis of 2-(nicotinamido)ethyl (*S*)-1-(benzylsulfonyl)piperidine-2-carboxylate (**1**) and 2-(nicotinamido)ethyl (*S*)-piperidine-2-carboxylate

(**12**) was according to Seufert et al.[19] Synthesis of lead structures (*S*)-1-Oxo-3-phenyl-1-((pyridin-3-ylmethyl)amino)propan-2-yl (*S*)-1-(benzylsulfonyl)piperidine-2-carboxylate (*S,S*-**2**), (*R*)-1-Oxo-3-phenyl-1-((pyridin-3-ylmethyl)amino)propan-2-yl (*S*)-1-(benzylsulfonyl)piperidine-2-carboxylate (*S,R*-**2**), (*R*)-1-Oxo-3-phenyl-1-((pyridin-3-ylmethyl)amino)propan-2-yl (*R*)-1-(benzylsulfonyl) piperidine-2-carboxylate (*R,R*-**2**), (*S*)-1-Oxo-3-phenyl-1-((pyridin-3-ylmethyl)amino)propan-2-yl (*R*)-1-(benzylsulfonyl)piperidine-2-carboxylate (*R,S*-**2**) and (*S*)-1-((4-Fluorobenzyl)sulfonyl)-*N*-((*S*)-4-methyl-1-oxo-1-((pyridin-3-ylmethyl)-amino)-pentan-2-yl)piperidine-2-carboxamide (**3a**) has been described by Scheuplein et al.[18]

General Procedures

General Procedure A: Amidation

Amidation was carried out according to methods reported in the literature.[36] First, 1 equivalent of the limiting reactant (carboxylic acid or amine) was dissolved in dry DCM and/or DMF (4 – 20 mL per 1 mmol limiting reactant) and the corresponding coupling partner (1 – 1.2 equiv.) was added under ice cooling. HBTU (2 equiv.) served as coupling reagent, and an auxiliary base (DIPEA, or TEA; 1 – 4 equiv.) was added further. After stirring for 15 min, the reaction mixture was allowed to adopt rt and stirred to completion, which was monitored by TLC. Extraction was carried out with dilute HCl, followed by dilute $NaHCO_3$. After separation of the phases, the combined organic layers were dried over Na_2SO_4 and filtered. The organic solvent was removed *in vacuo*, and the crude product was purified by column chromatography.

General Procedure B: Boc-Deprotection

According to Seufert et al.[19] the Boc-protecting group was removed at rt with an excess of TFA (2 – 5 mL) in dry DCM (10-20 mL), with TFA initially added slowly and under ice cooling. After completion (2 h), the reaction was neutralized with a saturated $NaHCO_3$ solution and extracted. The aqueous phase was washed with chloroform (5 x 20 mL) and the combined organic layers were dried over Na_2SO_4, filtered, and the solvent was removed *in vacuo* to give the crude product, which was used without further purification.

General Procedure C: Synthesis of Sulfonamides

Following a modified procedure of Seufert et al.[19], TEA (1.5 – 3 equiv.) and the corresponding sulfonyl chloride (1 – 1.3 equiv.) were added to a solution of the piperidine derivative (1 equiv.) in dry DCM (15 mL per 1 mmol limiting reactant) under ice cooling. The reaction was then stirred at rt until complete conversion, which was monitored by TLC. The solvent was removed *in vacuo* and the residue was purified by column chromatography.

Fluorescence polarization assay

The FPA was performed as described in Scheuplein et al.[18] Two different fluorescent probes were used for the competitive assay, depending on the affinity and thus the competitiveness of the inhibitor. (The affinities of the probes to the MIP proteins, as well as their respective use in the competitive assay, are shown in the SI.) For the competitive *Bp*MIP assay, the same concentrations of probe and protein were used as described in Scheuplein et al.[18] In contrast, a higher protein concentration was required for *Tc*MIP and *Lp*MIP due to their lower binding affinities to both fluorescent probes For this reason, the final protein concentration for the competition assay in the well was increased to 2 µM for *Tc*MIP and 2 - 4 µM for *Lp*MIP. Each inhibitor was measured at least in triplicate. Raw data and SD are given in the SI.

A similar procedure was used to determine the affinities of the lead compounds (**3a**, **3b**) to the human FKBPs. The procedure is described in detail in Kozany et al.[34]

Galleria Mellonella Toxicity and Infection Assay

The moth larvae of *G. mellonella* were cultured as described elsewhere.[37] They were reared in-house and kept in the dark at 30 °C until use. The inhibitors were dissolved to a 50 mM stock solution in DMSO and diluted with PBS to concentrations of 100 µM and 500 µM. To prevent precipitation, the final concentration of DMSO was increased to 10 % (v/v). Five larvae were injected with 10 µL each of a 100 µM or 500 µM solution of the inhibitors (**5b**, **10**) or 10 % DMSO as a control, which were then kept isolated at 37 °C in the dark. The survival rate was monitored over a period of 5 days according to Sprynski et al.[37] To assess the effect of MIP inhibitors on *B. thailandensis* pathogenicity, a dilution of $5x10^4$ CFU/10 µL *B. thailandensis* in PBS was prepared. Groups of 10 larvae were treated with 10 µL of *B. thailandensis* or PBS. Two hours after infection, the larvae were treated with a combination of cotrimoxazole at a dose of 10 mg/kg and diluent (water) or a combination with 250 µM of the MIP inhibitor **10**.[25] The final concentration of DMSO was 10 % in each case. After 20 hours, survival was monitored every second hour and Kaplan-Meier survival curves were obtained from three independent experiments.

Protease-coupled PPIase assay

Recombinant *Bp*MIP was expressed and purified as per Iwasaki et al.[10] The protease-coupled PPIase assay was conducted as per Fischer et al.[38] In brief, 400 nM inhibitor was co-incubated with *Bp*MIP and the substrate succinyl-Ala-Phe-Pro-Phe-*p*-nitroanilide (10 mg/mL, SAPPP, Bachem) in a glass cuvette at 4°C for six minutes prior to the addition of the protease α-chymotrypsin (SigmaAldrich, Merck). Cleavage of the chromophore, *p*-nitroanilide was measured at 390 nm at two second intervals for 900 seconds using a Shimadzu 1800 UV/Vis spectrophotometer. Enzymes assays were conducted in triplicate on different days and the average observed rate constant (K_{obs}) determined.

Computational methods

Protein setup: The details of the *Tc*MIP purification and structure determination are described in the accompanying paper.[26] The structure is available from the PDB (8P42).[26] For computational studies, the structure was prepared with MOE[39] (version 2022.02). The terminal residues Ala4 and Asp135 were capped and protonation was conducted with the *Protonate3D*[40] functionality at pH = 7.4. For dockings, ligand and water molecules were removed. For MD simulations, water molecules with a B-factor < 30 Å² were kept.

Ligand setup: The inhibitors shown in **Figure 2** were manually built in MOE. Energy minimization was carried out with the MMFF94x force field to a gradient of 0.001 kcal·mol^{-1}·Å^{-1}.

Docking calculations were performed with GOLD[41] (version 2023.1.0). For every inhibitor, 50 docking poses were generated with each of the implemented scoring functions ASP[42], Chemscore[43, 44], ChemPLP[45] and Goldscore[46] at 200 % search efficiency. The binding site was defined as a sphere with 12 Å radius centered between residues Trp94, Phe85 and Tyr117. A weak constraint was applied according to our previous studies[19] to favor docking poses that form a hydrogen bond with the backbone NH group of Ile91 (referring to *Tc*MIP). The obtained docking poses were rescored with DSX[47] using potentials derived from the Cambridge Structural Database[48]. Additionally, RMSD values were calculated to the N-sulfonyl-pipecolic acid core of compound CJ168 in the superposed *Bp*MIP crystal structure 4G50[49] to assess the compliance of the generated docking poses with the current binding hypothesis. For subsequent MD simulations, the best scored pose according to DSX among all poses with core RMSD ≤ 1 Å was selected. If no such pose was obtained, the pose with lowest core RMSD was selected.

Molecular dynamics simulations were performed with Desmond[27, 28] and the OPLS4 force field[29] (Schrödinger release 2023-2). Bond orders were reassigned, and hydrogen atom positioning was optimized for the protein structure in the Maestro suite. The selected docking pose was added to the respective complex before the *System Builder* tool was used to neutralize and to solvate the system in an orthorhombic box with 10 Å distance between protein and box border in every direction. Three replicas of 100 ns NPT runs were simulated at default settings with randomly selected seeds (cf. Supporting Information for further details). The obtained trajectories were converted to dcd format with VMD[50] before geometric analyses were carried out with Amber CPPTRAJ[51].

Quantum-mechanical calculations of the electrostatic surface potential at the density functional theory (DFT) level were performed with Gaussian16[52] for the truncated N-methyl-amide substructures of the chlorine or bromine containing inhibitors. The B3LYP functional was applied with the basis set 6-311+G**. Geometry optimization was enabled. Visualization was conducted with PyMol[53] with the electron density isosurface set to 0.001 au.

Abbreviations

au, atomic units; ASP, Astex Statistical Potential; B3LYP, Becke 3-parameter Lee–Yang–Parr; Boc, *tert*-butyloxycarbonyl; *Bp., Burkholderia pseudomallei; Bp*MIP, *Burkholderia pseudomallei* MIP; CFU, colony forming unit; ChemPLP, ChemScore Piecewise Linear Potential; m-CPBA, *meta*-chloroperbenzoic acid; DCM, dichlormethane; DIPEA, *N,N*-diisopropylethylamine; DMF, dimethylformamide; DMSO, Dimethyl sulfoxide; DSX, Drugscore eXtended; EA, ethyl acetate; FA, formic acid; FKBP, FK506 binding protein; FPA, fluorescence polarization assay; GOLD, Genetic Optimisation for Ligand Docking; HBTU, hexafluorophosphate benzotriazole tetramethyl uronium; K_D, dissociation constant; K_i, inhibition constant; K_{obs}, observed rate constant; LLC-MK_2, Rhesus Monkey Kidney Epithelial; *Lp*, *Legionella pneumophila*; *Lp*MIP, *Legionella pneumophila* MIP; MD, molecular dynamics; MeOH, methanol; MIP, macrophage infectivity potentiator; MOE, Molecular Operating Environment; NB, no binding; NPT, isothermal-isobaric ensemble; PBS, Phosphate-buffered saline; PPIase, peptidyl-prolyl *cis-trans* isomerase; RMSD, root mean square deviation of atomic positions; rt, room temperature; *Tc*, *Trypanosoma cruzi*; *Tc*MIP, *Trypanosoma cruzi* MIP; TEA, triethylamine; TFA, trifluoroacetic acid; VMD, Visual Molecular Dynamics

Author Information

Corresponding Author

U.H.: email, ulrike.holzgrabe@uni-wuerzburg.de

ORCID

Theresa Lohr: 0000-0001-6473-0983

Carina Herbst: 0009-0008-0247-7124

Nicole M Bzdyl: 0000-0003-2204-1172

Nicolas J. Scheuplein: 0000-0003-3261-7964

Jacob J. Whittaker: 0000-0001-8966-111X

Albert Guskov: 0000-0003-2340-2216

Felix Hausch: 0000-0002-3710-8838

Ute A. Hellmich: 0000-0001-7162-285X

Christoph Sotriffer 0000-0003-4713-4068

Ulrike Holzgrabe: 0000-0002-0364-7278

Author Contributions

‡ T.L. Writing - Original Draft, Methodology, Investigation, Formal analysis

C.H. Writing - Original Draft, Software, Formal analysis

N.M.B. Investigation

C.J. and I.N. Investigation
N.J.S. Methodology
W.O.S. Investigation
J.J.W. Investigation
A.G. Investigation
U.A.H. Writing - Review & Editing
F.H. Writing - Review & Editing
M.S-T. Writing - Review & Editing
C.S. Writing - Review & Editing, Supervision
U.H. Writing - Review & Editing, Supervision, Conceptualization

Declaration of competing interest

The authors declare that they have no known competing financial interests or personal relationships that could have appeared to influence the work reported in this paper.

Acknowledgement

Laura Backer and Lukas Kirchner is thanked for providing the HRMS data.

References

1. Scheuplein, N. J.; Bzdyl, N. M.; Kibble, E. A.; Lohr, T.; Holzgrabe, U.; Sarkar-Tyson, M., Targeting Protein Folding: A Novel Approach for the Treatment of Pathogenic Bacteria. *J. Med. Chem.* **2020,** *63* (22), 13355-13388.doi. 10.1021/acs.jmedchem.0c00911
2. Humbert, M. V.; Almonacid Mendoza, H. L.; Jackson, A. C.; Hung, M. C.; Bielecka, M. K.; Heckels, J. E.; Christodoulides, M., Vaccine potential of bacterial macrophage infectivity potentiator (MIP)-like peptidyl prolyl cis/trans isomerase (PPIase) proteins. *Expert Rev. Vaccines* **2015,** *14* (12), 1633-49.doi. 10.1586/14760584.2015.1095638
3. Ünal, C. M.; Steinert, M., Microbial peptidyl-prolyl cis/trans isomerases (PPIases): virulence factors and potential alternative drug targets. *Microbiol. Mol. Biol. Rev.* **2014,** *78* (3), 544-71.doi. 10.1128/MMBR.00015-14
4. Rasch, J.; Unal, C. M.; Klages, A.; Karsli, U.; Heinsohn, N.; Brouwer, R.; Richter, M.; Dellmann, A.; Steinert, M., Peptidyl-Prolyl-cis/trans-Isomerases Mip and PpiB of Legionella pneumophila Contribute to Surface Translocation, Growth at Suboptimal Temperature, and Infection. *Infect. Immun.* **2019,** *87* (1).doi. 10.1128/IAI.00939-17
5. Cianciotto, N. P.; Eisenstein, B. I.; Mody, C. H.; Toews, G. B.; Engleberg, N. C., A Legionella pneumophila gene encoding a species-specific surface protein potentiates initiation of intracellular infection. *Infect. Immun.* **1989,** *57* (4), 1255-62.doi. 10.1128/iai.57.4.1255-1262.1989
6. Norville, I. H.; Harmer, N. J.; Harding, S. V.; Fischer, G.; Keith, K. E.; Brown, K. A.; Sarkar-Tyson, M.; Titball, R. W., A Burkholderia pseudomallei macrophage infectivity potentiator-like protein has rapamycin-inhibitable peptidylprolyl isomerase activity and pleiotropic effects on virulence. *Infect. Immun.* **2011,** *79* (11), 4299-307.doi. 10.1128/IAI.00134-11
7. Norville, I. H.; Breitbach, K.; Eske-Pogodda, K.; Harmer, N. J.; Sarkar-Tyson, M.; Titball, R. W.; Steinmetz, I., A novel FK-506-binding-like protein that lacks peptidyl-prolyl isomerase activity is involved in intracellular infection and in vivo virulence of Burkholderia pseudomallei. *Microbiology* **2011,** *157* (Pt 9), 2629-2638.doi. 10.1099/mic.0.049163-0
8. Reimer, A.; Seufert, F.; Weiwad, M.; Ebert, J.; Bzdyl, N. M.; Kahler, C. M.; Sarkar-Tyson, M.; Holzgrabe, U.; Rudel, T.; Kozjak-Pavlovic, V., Inhibitors of macrophage infectivity potentiator-like PPIases affect neisserial and chlamydial pathogenicity. *Int. J. Antimicrob. Agents* **2016,** *48* (4), 401-8.doi. 10.1016/j.ijantimicag.2016.06.020
9. Debowski, A. W.; Bzdyl, N. M.; Thomas, D. R.; Scott, N. E.; Jenkins, C. H.; Iwasaki, J.; Kibble, E. A.; Khoo, C. A.; Scheuplein, N. J.; Seibel, P. M.; Lohr, T.; Metters, G.; Bond, C. S.; Norville, I. H.; Stubbs, K. A.; Harmer, N. J.; Holzgrabe, U.; Newton, H. J.; Sarkar-Tyson, M., Macrophage infectivity potentiator protein, a peptidyl prolyl cis-trans isomerase, essential for Coxiella burnetii growth and pathogenesis. *PLoS Pathog.* **2023,** *19* (7), e1011491.doi. 10.1371/journal.ppat.1011491
10. Iwasaki, J.; Lorimer, D. D.; Vivoli-Vega, M.; Kibble, E. A.; Peacock, C. S.; Abendroth, J.; Mayclin, S. J.; Dranow, D. M.; Pierce, P. G.; Fox, D.; Lewis, M.; Bzdyl, N. M.; Kristensen, S. S.; Inglis, T. J. J.; Kahler, C. M.; Bond, C. S.; Hasenkopf, A.; Seufert, F.; Schmitz, J.; Marshall, L. E.; Scott, A. E.; Norville, I. H.; Myler, P. J.; Holzgrabe, U.; Harmer, N. J.; Sarkar-Tyson, M., Broad-spectrum in vitro activity of macrophage infectivity potentiator inhibitors against Gram-negative bacteria and Leishmania major. *J. Antimicrob. Chemother.* **2022,** *77* (6), 1625-1634.doi. 10.1093/jac/dkac065
11. Pereira, P. J.; Vega, M. C.; Gonzalez-Rey, E.; Fernandez-Carazo, R.; Macedo-Ribeiro, S.; Gomis-Ruth, F. X.; Gonzalez, A.; Coll, M., Trypanosoma cruzi macrophage infectivity potentiator has a rotamase core and a highly exposed alpha-helix. *EMBO Rep.* **2002,** *3* (1), 88-94.doi. 10.1093/embo-reports/kvf009

12. Bern, C.; Kjos, S.; Yabsley, M. J.; Montgomery, S. P., Trypanosoma cruzi and Chagas' Disease in the United States. *Clin. Microbiol. Rev.* **2011,** *24* (4), 655-81.doi. 10.1128/CMR.00005-11
13. Bern, C., Chagas' disease. *N. Engl. J. Med.* **2015,** *373* (5), 456-466.
14. Moro, A.; Ruiz-Cabello, F.; Fernandez-Cano, A.; Stock, R. P.; Gonzalez, A., Secretion by Trypanosoma cruzi of a peptidyl-prolyl cis-trans isomerase involved in cell infection. *EMBO J.* **1995,** *14* (11), 2483-90.doi. 10.1002/j.1460-2075.1995.tb07245.x
15. Schreiber, S. L., Chemistry and biology of the immunophilins and their immunosuppressive ligands. *Science* **1991,** *251* (4991), 283-7.doi. 10.1126/science.1702904
16. Pomplun, S.; Sippel, C.; Hahle, A.; Tay, D.; Shima, K.; Klages, A.; Unal, C. M.; Riess, B.; Toh, H. T.; Hansen, G.; Yoon, H. S.; Bracher, A.; Preiser, P.; Rupp, J.; Steinert, M.; Hausch, F., Chemogenomic Profiling of Human and Microbial FK506-Binding Proteins. *J. Med. Chem.* **2018,** *61* (8), 3660-3673.doi. 10.1021/acs.jmedchem.8b00137
17. Wiedemann, C.; Whittaker, J. J.; Perez Carrillo, V. H.; Goretzki, B.; Dajka, M.; Tebbe, F.; Harder, J.-M.; Krajczy, P.; Joseph, B.; Hausch, F., Legionella pneumophila macrophage infectivity potentiator protein appendage domains modulate protein dynamics and inhibitor binding. *bioRxiv* **2023**, 2023.04. 24.538046.
18. Scheuplein, N. J.; Bzdyl, N. M.; Lohr, T.; Kibble, E. A.; Hasenkopf, A.; Herbst, C.; Sarkar-Tyson, M.; Holzgrabe, U., Analysis of Structure-Activity Relationships of Novel Inhibitors of the Macrophage Infectivity Potentiator (Mip) Proteins of Neisseria meningitidis, Neisseria gonorrhoeae, and Burkholderia pseudomallei. *J. Med. Chem.* **2023**.doi. 10.1021/acs.jmedchem.3c00458
19. Seufert, F.; Kuhn, M.; Hein, M.; Weiwad, M.; Vivoli, M.; Norville, I. H.; Sarkar-Tyson, M.; Marshall, L. E.; Schweimer, K.; Bruhn, H.; Rosch, P.; Harmer, N. J.; Sotriffer, C. A.; Holzgrabe, U., Development, synthesis and structure-activity-relationships of inhibitors of the macrophage infectivity potentiator (Mip) proteins of Legionella pneumophila and Burkholderia pseudomallei. *Bioorg. Med. Chem.* **2016,** *24* (21), 5134-5147.doi. 10.1016/j.bmc.2016.08.025
20. Scheuplein, N. J.; Lohr, T.; Vivoli Vega, M.; Ankrett, D.; Seufert, F.; Kirchner, L.; Harmer, N. J.; Holzgrabe, U., Fluorescent probe for the identification of potent inhibitors of the macrophage infectivity potentiator (Mip) protein of Burkholderia pseudomallei. *SLAS Discov.* **2023**.doi. 10.1016/j.slasd.2023.03.004
21. Wang, Z.-X., An exact mathematical expression for describing competitive binding of two different ligands to a protein molecule. *FEBS Lett.* **1995,** *360* (2), 111-114.doi. 10.1016/0014-5793(95)00062-e
22. Juli, C.; Sippel, M.; Jager, J.; Thiele, A.; Weiwad, M.; Schweimer, K.; Rosch, P.; Steinert, M.; Sotriffer, C. A.; Holzgrabe, U., Pipecolic acid derivatives as small-molecule inhibitors of the Legionella MIP protein. *J. Med. Chem.* **2011,** *54* (1), 277-83.doi. 10.1021/jm101156y
23. Lohr, T.; Scheuplein, N. J.; Jenkins, C.; Norville, I.; Erk, C.; Stapf, M.; Kirchner, L.; Sarkar-Tyson, M.; Holzgrabe, U., Identification of active main metabolites of anti-infective inhibitors of the macrophage infectivity potentiator protein by liquid chromatography using mass detection. *Arch. Pharm. (Weinheim)* **2024**, e2400032.doi. 10.1002/ardp.202400032
24. Kovacs-Simon, A.; Hemsley, C.; Scott, A.; Prior, J.; Titball, R., Burkholderia thailandensis strain E555 is a surrogate for the investigation of Burkholderia pseudomallei replication and survival in macrophages. *BMC Microbiol.* **2019,** *19*, 1-16.
25. Thomas, R. J.; Hamblin, K. A.; Armstrong, S. J.; Müller, C. M.; Bokori-Brown, M.; Goldman, S.; Atkins, H. S.; Titball, R. W., Galleria mellonella as a model system to test the pharmacokinetics and efficacy of antibiotics against Burkholderia pseudomallei. *Int. J. Antimicrob. Agents* **2013,** *41* (4), 330-336.

26. Pérez Carrillo, V. H., Whittaker, J.J., Wiedemann, C., Harder, J.-M., Lohr, T., Jamithireddy, A., Dajka, M., Goretzki, B., Joseph, B., Guskov, A., Harmer, N., Holzgrabe, U., Hellmich, U.A., Structure and dynamics of macrophage infectivity potentiator proteins from pathogenic bacteria and protozoans bound to fluorinated pipecolic acid inhibitors. *Eur. J. Med. Chem. submitted*.
27. Release, S., 1: Desmond Molecular Dynamics System, DE Shaw Research, New York, NY, 2021. Maestro-Desmond Interoperability Tools, Schrödinger. 2023.
28. Bowers, K. J.; Sacerdoti, F. D.; Salmon, J. K.; Shan, Y.; Shaw, D. E.; Chow, E.; Xu, H.; Dror, R. O.; Eastwood, M. P.; Gregersen, B. A.; Klepeis, J. L.; Kolossvary, I.; Moraes, M. A., Scalable algorithms for molecular dynamics simulations on commodity clusters.doi. 10.1145/1188455.1188544
29. Lu, C.; Wu, C.; Ghoreishi, D.; Chen, W.; Wang, L.; Damm, W.; Ross, G. A.; Dahlgren, M. K.; Russell, E.; Von Bargen, C. D., OPLS4: Improving force field accuracy on challenging regimes of chemical space. *J. Chem. Theory Comput.* **2021,** *17* (7), 4291-4300.
30. Bissantz, C.; Kuhn, B.; Stahl, M., A medicinal chemist's guide to molecular interactions. *J. Med. Chem.* **2010,** *53* (14), 5061-5084.
31. Wilcken, R.; Zimmermann, M. O.; Lange, A.; Joerger, A. C.; Boeckler, F. M., Principles and applications of halogen bonding in medicinal chemistry and chemical biology. *J. Med. Chem.* **2013,** *56* (4), 1363-1388.
32. Kolar, M. H.; Hobza, P., Computer modeling of halogen bonds and other σ-hole interactions. *Chem. Rev.* **2016,** *116* (9), 5155-5187.
33. Bauder, M.; Meyners, C.; Purder, P. L.; Merz, S.; Sugiarto, W. O.; Voll, A. M.; Heymann, T.; Hausch, F., Structure-based design of high-affinity macrocyclic FKBP51 inhibitors. *J. Med. Chem.* **2021,** *64* (6), 3320-3349.
34. Kozany, C.; Marz, A.; Kress, C.; Hausch, F., Fluorescent probes to characterise FK506-binding proteins. *ChemBioChem* **2009,** *10* (8), 1402-10.doi. 10.1002/cbic.200800806
35. Hiltensperger, G.; Hecht, N.; Kaiser, M.; Rybak, J. C.; Hoerst, A.; Dannenbauer, N.; Muller-Buschbaum, K.; Bruhn, H.; Esch, H.; Lehmann, L.; Meinel, L.; Holzgrabe, U., Quinolone Amides as Antitrypanosomal Lead Compounds with In Vivo Activity. *Antimicrob. Agents Chemother.* **2016,** *60* (8), 4442-52.doi. 10.1128/AAC.01757-15
36. Goodreid, J. D.; Duspara, P. A.; Bosch, C.; Batey, R. A., Amidation reactions from the direct coupling of metal carboxylate salts with amines. *J. Org. Chem.* **2014,** *79* (3), 943-54.doi. 10.1021/jo402374c
37. Sprynski, N.; Valade, E.; Neulat-Ripoll, F., Galleria mellonella as an infection model for select agents. *Methods Mol. Biol.* **2014,** *1197*, 3-9.doi. 10.1007/978-1-4939-1261-2_1
38. Fischer, G.; Bang, H.; Mech, C., [Determination of enzymatic catalysis for the cis-trans-isomerization of peptide binding in proline-containing peptides]. *Biomed Biochim Acta* **1984,** *43* (10), 1101-1111.
39. Ulc, C. C. G. *Molecular Operating Environment (MOE), 2022.02*, 1010 Sherbooke St. West, Suite #910, Montreal, QC, Canada, H3A 2R7, 2023.
40. Labute, P., Protonate3D: assignment of ionization states and hydrogen coordinates to macromolecular structures. *Proteins: Struct., Funct., Bioinf.* **2009,** *75* (1), 187-205.
41. Jones, G.; Willett, P.; Glen, R. C., A genetic algorithm for flexible molecular overlay and pharmacophore elucidation. *J. Comput.-Aided Mol. Des.* **1995,** *9*, 532-549.
42. Mooij, W. T.; Verdonk, M. L., General and targeted statistical potentials for protein–ligand interactions. *Proteins: Struct., Funct., Bioinf.* **2005,** *61* (2), 272-287.
43. Eldridge, M. D.; Murray, C. W.; Auton, T. R.; Paolini, G. V.; Mee, R. P., Empirical scoring functions: I. The development of a fast empirical scoring function to estimate the binding affinity of ligands in receptor complexes. *J. Comput.-Aided Mol. Des.* **1997,** *11*, 425-445.

44. Baxter, C. A.; Murray, C. W.; Clark, D. E.; Westhead, D. R.; Eldridge, M. D., Flexible docking using Tabu search and an empirical estimate of binding affinity. *Proteins: Struct., Funct., Bioinf.* **1998,** *33* (3), 367-382.
45. Korb, O.; Stutzle, T.; Exner, T. E., Empirical scoring functions for advanced protein− ligand docking with PLANTS. *J. Chem. Inf. Model.* **2009,** *49* (1), 84-96.
46. Jones, G.; Willett, P.; Glen, R. C., Molecular recognition of receptor sites using a genetic algorithm with a description of desolvation. *J. Mol. Biol.* **1995,** *245* (1), 43-53.
47. Neudert, G.; Klebe, G., DSX: a knowledge-based scoring function for the assessment of protein–ligand complexes. *J. Chem. Inf. Model.* **2011,** *51* (10), 2731-2745.
48. Allen, F. H., The Cambridge Structural Database: a quarter of a million crystal structures and rising. *Acta Crystallogr. B.* **2002,** *58* (3), 380-388.
49. Begley, D. W.; Fox, D., 3rd; Jenner, D.; Juli, C.; Pierce, P. G.; Abendroth, J.; Muruthi, M.; Safford, K.; Anderson, V.; Atkins, K.; Barnes, S. R.; Moen, S. O.; Raymond, A. C.; Stacy, R.; Myler, P. J.; Staker, B. L.; Harmer, N. J.; Norville, I. H.; Holzgrabe, U.; Sarkar-Tyson, M.; Edwards, T. E.; Lorimer, D. D., A structural biology approach enables the development of antimicrobials targeting bacterial immunophilins. *Antimicrob. Agents Chemother.* **2014,** *58* (3), 1458-67.doi. 10.1128/AAC.01875-13
50. Humphrey, W.; Dalke, A.; Schulten, K., VMD: visual molecular dynamics. *J. Mol. Graphics Modell.* **1996,** *14* (1), 33-38.
51. Roe, D. R.; Cheatham III, T. E., PTRAJ and CPPTRAJ: software for processing and analysis of molecular dynamics trajectory data. *J. Chem. Theory Comput.* **2013,** *9* (7), 3084-3095.
52. Frisch, M. J.; Trucks, G. W.; Schlegel, H. B.; Scuseria, G. E.; Robb, M. A.; Cheeseman, J. R.; Scalmani, G.; Barone, V.; Petersson, G. A.; Nakatsuji, H.; Li, X.; Caricato, M.; Marenich, A. V.; Bloino, J.; Janesko, B. G.; Gomperts, R.; Mennucci, B.; Hratchian, H. P.; Ortiz, J. V.; Izmaylov, A. F.; Sonnenberg, J. L.; Williams; Ding, F.; Lipparini, F.; Egidi, F.; Goings, J.; Peng, B.; Petrone, A.; Henderson, T.; Ranasinghe, D.; Zakrzewski, V. G.; Gao, J.; Rega, N.; Zheng, G.; Liang, W.; Hada, M.; Ehara, M.; Toyota, K.; Fukuda, R.; Hasegawa, J.; Ishida, M.; Nakajima, T.; Honda, Y.; Kitao, O.; Nakai, H.; Vreven, T.; Throssell, K.; Montgomery Jr, J. A.; Peralta, J. E.; Ogliaro, F.; Bearpark, M. J.; Heyd, J. J.; Brothers, E. N.; Kudin, K. N.; Staroverov, V. N.; Keith, T. A.; Kobayashi, R.; Normand, J.; Raghavachari, K.; Rendell, A. P.; Burant, J. C.; Iyengar, S. S.; Tomasi, J.; Cossi, M.; Millam, J. M.; Klene, M.; Adamo, C.; Cammi, R.; Ochterski, J. W.; Martin, R. L.; Morokuma, K.; Farkas, O.; Foresman, J. B.; Fox, D. J. *Gaussian 16 Rev. B.01*, Wallingford, CT, 2016.
53. Schrodinger, L. L. C., The PyMOL Molecular Graphics System, Version 2.4.1. **2020**.